Original Article
DOI: https://doi.org/10.70749/ijbr.v2i02.429

INDUS JOURNAL OF BIOSCIENCE RESEARCH
https://induspublishers.com/IJBR
ISSN: 2960-2793/ 2960-2807

Crossref

OPEN ACCESS

Solar Photocatalytic Removal of Natural Organic Matter using Fluorinated Calcium Zincate Grafted on Gravel

Tahseen Anwer[1], Iqra Shahzadi[2], Syed Anwaar Hussain Shah[3], Amna Nasir[1], Arslan Khan[4], Maryam iqbal[5], Sayeda Nimra jabeen[6], Muhammad Rizwan Javed[7], Wasifa[1], Syed Muneeb ur Rehman[7]

[1]Department of Chemistry, University of Agriculture, Faisalabad, Punjab, Pakistan.
[2]College of Earth and Environmental Sciences, University of the Punjab, Lahore, Punjab, Pakistan.
[3]Department of Physics, University of Agriculture, Faisalabad, Punjab, Pakistan.
[4]Department of Environmental Sciences, The University of Lahore, Punjab, Pakistan.
[5]Department of Biochemistry, Abdul Wali Khan University Mardan, KP, Pakistan.
[6]Department of Chemistry, Government College Women University, Faisalabad, Punjab, Pakistan
[7]Center of Excellence in Solid State Physics, University of the Punjab, Lahore, Punjab, Pakistan.

ARTICLE INFO

Keywords
Solar photocatalysis, Fluorinated calcium zincate, Gravel-supported catalysts, Water treatment, Environmental sustainability.

Corresponding Author: Tahseen Anwer, Department of Chemistry, University of Agriculture, Faisalabad, Punjab, Pakistan.
Email: tahseenanwer244@gmail.com

Declaration

Author's Contributions: All authors contributed to the study and approved the final manuscript.
Conflict of Interest: The authors declare no conflict of interest.
Funding: No funding was received.

Article History

Received: 17-10-2024
Revised: 05-12-2024
Accepted: 19-12-2024

ABSTRACT

Natural organic matter issue (NOM) is a delegated class of harmful poisons in water that must be evacuated by utilizing efficient and eco-accommodating treatment procedures to chop down water contamination. In this, a composite of the evacuation of NOM utilizing fluorinated and non-fluorinated calcium zincate composite joined over rock by splash pyrolysis technique was accounted for. The created material was portrayed by checking electron microscopy, vitality dispersive X-beam, Fourier change infrared spectroscopy and X-beam diffraction spectroscopy. Response parameters like starting centralization of NOM and oxidant (H2O2), introductory pH and light time were improved utilizing the Reaction surface technique (RSM). Later, photocatalytic movement of fluorinated/non-fluorinated calcium zincate under conditions streamlined by RSM to debase NOM in city wastewater upon daylight presentation was resolved. NOM's degree of debasement was estimated using UV/noticeable spectrophotometer, Fourier change infrared spectroscopy (FTIR) and elite fluid chromatography (HPLC). Water quality parameters, such as natural oxygen request, substance oxygen request, and aggregate natural carbon, were resolved. Treated wastewater can be reused for water systems, washing and mechanical procedures.

INTRODUCTION

Many organic and inorganic substances, such as heavy metals and biological pollutants, are reported in water, making it toxic, dangerous, and carcinogenic for all life on land (Borah et al., 2020). In industrial countries, it is compulsory to control the discharge of these hazardous and toxic substances, even at low concentrations. In industrial countries, preventing the discharge of these dangerous and poisonous substances is mandatory, even at low concentrations (Saravanan *et al.*, 2021). The basic reasons for increasing pollution are insufficient sanitation, detergents, pesticides, fertilizer, chemicals, toxic metals and natural organic matter, and industrial, agricultural and domestic waste material residues. These contaminants and pollutants change water's

chemical, biological, and physical characteristics (Ahmed *et al.*, 2021). Natural organic matter (NOM) is a group of heterogeneous macromolecules with aliphatic and aromatic hydrocarbon structures and varying molecular weights and functional groups (Sievert *et al.*, 2011). NOM is found in water and is formed by the breakdown of dead and decayed material of plants and animals, which melt badly and give a bitter taste in water. NOM comprises hydrophilic and hydrophobic components (Owodunni et al., 2021). Disinfectants, such as trihalomethane and lactic acids, produce carcinogenic disinfection by-products during water treatment (Dad et al., 2018).

Hopeful Future: The extensive investigation into the removal of NOM and the use of various treatment technologies such as chemical, biological, and physical methods like nano-filtration, enhanced coagulation, biodegradation, adsorption, ultrafiltration, and chemical oxidation processes, offers hope for a cleaner and safer future. Our research on the solar photocatalytic removal of NOM using fluorinated calcium zincate grafted on gravel is a significant step toward this future, offering a promising solution to water pollution. (Anwar et al., 2024), biodegradation, adsorption, ultrafiltration and chemical oxidation processes are used to remove NOM from wastewater (Acero et al., 2016). The advanced oxidation process (AOP) is an alternative method that completely degrades numerous organic pollutants. Its effectiveness is based on creating reactive species (H2O2, OH°, O2 and O3) for mineralizing disinfection by-products, water pathogens and refectory organic compounds. This method, with its ability to generate less toxic intermediate products during the degradation of organic pollutants, is a reliable and efficient tool in our research. (Bethi *et al.*, 2016). AOPs can generate less toxic intermediate products during the degradation of organic pollutants. Among the various transition metal oxides applied as nano photocatalysts, nano Zinc oxide is the preferable material as compared to others because it has unique chemical properties as well as physical properties like high chemical stability, high photostability, optical and chemical properties, harvesting of a wide range of solar radiation, electrochemical is also high, and cost-effective.

The visible portion, the main component of solar radiation, can effectively establish a stable photocatalytic system. To overcome the limitations of the band gap, many studies on coupled semiconductor photocatalysts like ZnO-TiO_2, CuO-ZnO, CuO-TiO_2, CuO-SnO_2, TiO_2-SnO_2 and ZnO-SnO_2 etc. have been reported (Sharma et al., 2024). A composite of Zinc oxide and Calcium oxide decreases the band gap from 3.38 to nearly 2.9 eV by enhancing electron-hole pair separation. The resultant decrease in crystal size and absorption shift from the ultraviolet to the visible region. Fluorination of calcium zincate leads to a greater oxidation rate by trapping surface electrons. Various studies have been carried out on preparing calcium zincate using different methods such as the sol-gel method, hydrothermal method, and co-precipitation method. However, the methods require specific conditions, such as a quality substrate and sensitive apparatus. Considering the limitations of other methods, the present work has been designed to grow fluorinated calcium zincate on gravel material by spray pyrolysis method, which was used for the photocatalytic degradation of NOM in municipal wastewater under operational parameters optimized by RSM.

MATERIAL AND METHODS

The research was conducted in the Radiation Chemistry Lab and general labs of the Department of Chemistry, University of Agriculture, Faisalabad, under the supervision of Prof. Dr. Ijaz Ahmed Bhatti. These labs have state-of-the-art facilities and a long-standing reputation for conducting high-quality research in environmental chemistry and water treatment.

Synthetic Concoctions Required

Sodium hydroxide (Merck), Potassium hydroxide (Merck), Ammonium fluoride (Merck), Zinc Acetate dry out (Daejung), Calcium chloride dihydrate (Daejung), Sulphuric corrosive (Merck), Hydrogen peroxide (Merck), Potassium dichromate (Daejung), Zinc Sulfate heptahydrate (Daejung), Hydrochloric Acid (Merck), Mercury Sulfate (Daejung), Silver sulfate (Daejung), Glucose (Merck), Potassium hydrogen phthalate (Merck), Distil water

Apparatus and Glassware

Beakers (1000ml, 500ml, 400ml, 250ml, 100ml), Measuring chamber (100ml, 50ml, 10ml), Filter paper, Funnel, Thermometer, measuring chamber, Pipette 1ml, 2 ml, 5 ml and 10 ml, Apendroff tubes 1000 small scale litter, Test tubes, Aluminium thwart, Test tube stand, Test tube washing brush, Clamp stand, Tripod stand**,** Bottles for capacity, Spatula, Cuvettes, COD vials, Measuring carafes 100ml, 250mL, 500mL and 1000 mL, Three necked round base carafe 1000ml

1nstrument used in Lab

balance, (Sartorius TE 214 S), Analytic Hot plate, UV-Visib1e Spectr0photometer (CE Cecil 720, Germany), Atomics Abs0rption Spectr0meter, Ph meter (Lovibonds Senso, Directl50, Germany)

Accumulation and Capacity of Wastewater Tests

Wastewater tests were gathered from the civil wastewater of a University lodging close to Raja Wala Deplete, Faisalabad, following a standard technique (Eaton et al., 2015). Already treated plastic containers (washed with refined water and soaked in 1 % HNO3 for 24 hrs) were utilized to gather the waste water tests.

METHODOLOGY

All exploration work contains the following advances.

The Growth of fluorinated nanocomposite (ZnO/CaO) on the rock.

Characterization of nanocomposites by utilizing diverse systems like SEM, EDX, XRD

Optimization of grouping of nanocomposite.

Optimization of the PH of the model compound.

optimization of oxidant fixation.

Optimization of Irradiation time utilized for corruption of characteristic natural issues.

Calculate the Percentage of debasement of normal, natural issues from civil wastewater.

Development of fluorinated nanocomposite (ZnO/CaO) on rock.

Reagents

All the reagents utilized throughout this investigation were taken from the Radiation Lab of the Department of Chemistry, University of Agriculture Faisalabad. They were used for diagnostic review and were utilized without encouraging cleansing. These reagents include ethanol, Zinc sulfate heptahydrate, Calcium chloride dihydrate, Sodium hydroxide, hydrochloric corrosive, Sulfuric corrosive, Hydrogen peroxide and ammonium fluoride.

Arrangement of Reagents answer for Fluorinated nanocomposite ZnO/CaO

Arrangement of 0.1 M Zinc sulfate arrangement: Arrangement of 0.05 M Zinc sulfate was set up by dissolving 7.2 g of zinc sulfate heptahydrate in 500 ml ethanol. Arrangement of 0.1 calcium chloride arrangement: Arrangement of 0.05 M calcium chloride was set up by dissolving 3.7 g of calcium chloride dihydrate in 500 ml ethanol. Arrangement of 3mM ammonium fluoride arrangement. A 3mM ammonium fluoride arrangement was set up by dissolving 0.055 g of ammonium fluoride in 500 ml ethanol. Combination of F/CaZnO2 nanomaterial. A combination of Fluorinated nanocomposite ZnO/Cao nanomaterial was done in the radiation science lab of the division of science, University of Agriculture Faisalabad, by utilizing ethanol, Zinc Sulfate heptahydrate (ZnSO4. 7H2O), ammonium (NH4F) and calcium chloride dihydrate (CaCl2 . 2H2O).

Technique for the union of Nanoscaled Fluorinated ZnO/CaO.

Shower pyrolysis was utilized to union the nanostructure using ZnSO4.7H2O (Sigma-Aldrich) and NaOH (Sigma-Aldrich). Fluid arrangement of ZnSO4.7H2O (0.1M), NaOH (0.2M) and FeSO4 (4 Mm) was arranged in refined water in partitioned measuring utensils and after that, cationic arrangement by blending zinc also, sodium arrangement in 1:10. Dopent have included cation arrangement (Fe: Cationic) in 4:100. Water was taken as the ionic arrangement and its temperature was neared to its breaking point (80 C^{o}) what's more, the clay material was taken as a substrate.

Instrumentation

Weighing was finished by utilizing investigative adjust (Sartorius TE 214 S), and spectrophotometer estimations were performed on the UV/Vis twofold bar spectrophotometer (CE Cecil 7200, Germany) at Radiati0n science lab; a splash machine was utilized for shower pyrolysis for the readiness of thin layer fluorinated calcium zincate (F/CaZnO2) and vacuum drying stove (Mammert VO 400) for warming the rock and

Furnace (Mammert VO 400) for calcination of the fluorinated nanocomposite were additionally executed at the Radiation science lab,

Advanced pH meter

During experimentation, an advanced pH meter after adjustment was utilized (Lovibond Senso Coordinate 150, Germany). The pH meter was adjusted using the standard cushion arrangements of pH 4, 7 and 10. Before each perusing, the terminal of the pH meter was washed with refined water and then dried with perfect tissue paper.

Figure 1

Expository Balance

Expository g was utilized to weigh the whole examination. Suppress Furnace The heater is outfitted with a working tube that fills in to help with the warming wires. Subsequently, the favorable position is that the heater can accomplish high warmth-up rates for the application advertised. A mute heater with a working reach from up to 1100 º C at the Radiation Science lab, a branch of the Science College of Agriculture, Faisalabad, was utilized to strengthen tests of as-incorporated Fe-doped ZnO. The example was put in the Furnace at 350º C for 2 hours in a warm, safe porcelain pot, the temp. Expanded steadily from room temperature to the alluring level. Tests were expelled from the heater at the point when the room temperature was recaptured.

Synthetic oxygen request (COD) meter

A computerized COD meter at the Radiation science lab, UAF, was utilized for the COD and TOC estimations. The COD meter was aligned with standard arrangements of known COD. Preceding every estimation, the vials of the COD meter were altogether washed with refined wa

Figure 2

Analytical balance (Sartorius TE 214 S)

Figure 3

Digital Muffle Furnace

Figure 4

COD meter (Lovibond PCCHECKIT COD vario with Lovibond incubator)

Biochemical oxygen demand (BOD) meter

A digital BOD meter (Lovibond Senso Direct 150) at the Radiation chemistry lab UAF was used for the BOD measurement. The BOD meter was calibrated with standard solutions of known BOD.

Figure 5

BOD meter (Lovibond Senso Direct 150)

Table 1

Concentration (ppm)	Wavelength (nm)	Absorbance
80	367.5	0.913
365.0	0.945	
361.0	0.965	
359.5	0.965	
355.0	1.05	
100	367.5	1.223
365.0	1.263	
361.0	1.273	
359.5	1.110	
355.0	1.280	

Assurance of degree of debasement of NOM in wastewater:

UV/ Vis Spectroscopy controlled the degree of debasement of NOM in metropolitan wastewater tests, and Fourier Transform Infrared Spectroscopy (FTab, UAF was utilized to take absorbance spectra of untreated and treated examples of city wastewater. Before treatment, the absorbance of wastewater tests was recorded, and after Treatment, the absorbance was estimated again. The rate of NOM debasement in wastewater tests was dictated by computing the distinction in absorbance. For the assurance of NOM substance in wastewater, absorbance was estimated at 254 nm, which adds up to the substance of humic substances (HSs); absorbance at 280 nm speaks to the aggregate aromaticity of HSs. Absorbance at 400 and 436 nm speaks to the shading evacuation for HSs.

Figure 6

Double beam UV/VIS Spectrophotometer (CE Cecil 7200, Germany)

Assurance of Percentage Corruption A standard arrangement of potassium hydrogen phthalate was set up by dissolving 425 mg KHP in 1L of deionized water. Standard arrangement of potassium hydrogen phthalate, 425 ppm

Calculation of COD

Standard factor = COD of standard KHP/Absorbance after hatching COD of test (mg/L) = Standard factor × Absorbance of test after hatching

Estimation of Biochemical Oxygen Demand (BOD)

The biochemical oxygen request was estimated using an aligned advanced BOD meter (Lovibond Senso Direct 150) at the Radiation science lab at UAF.

Procedure

Uncommon BOD estimating bottles were washed and flushed with deionized water. In the to start with, a bottle of 56 ml of standard deionized water was included as clear. The five jugs were loaded with the same volume of standard arrangements, 50-150 ppm of F3BS. Seven drops of Standard KOH arrangement were added to vials of jugs before topping them. At that point, they were put in their particular positions. The body meter was set for 5 days. Estimations of BOD were estimated after 5 days. After photocatalysis, treated arrangements were again subjected to a BOD meter, and abatement in BOD esteems was watched. At that point, a % decrease in BOD was

figured. The same method was used after the profluent tests.

Response Parameters

Response parameters are assumed to play a huge part in the proficiency of photocatalysts. The productivity of photocatalysts could be upgraded by improving these response parameters. This work utilized two kinds of response parameters: (I) Constant response parameters and (ii) Variable response parameters. Consistent response parameters Some response parameters are kept consistent.

Sunlight (40-45 C˚), Catalyst Loading, NOM concentration (60 ppm), Variable response parameters, pH, Time, Irradiation Time, and Variable parameters were enhanced with the assistance of a reaction surface system (RSM), utilizing a planned master (adaptation 7.0) Programming.

Use of Statistical Outline

Reaction Surface Methodology (RSM) utilizing Central Composite Design (CCD) was used to improve the operational parameters, such as pH, Oxidant (H2O2) focus and illumination time, keeping in mind the end goal of assessing the photograph reactant productivity of arranged petite organized photograph impetuses.

RESULTS AND DISCUSSION

The Growth of Flourine doped $CaZnO_2$ Nanoparticles on Ceramic

In this examination, Nanoparticles of Fluorine doped ZnO were developed on Ceramic substrate by progressive ionic layer adsorption and response (SILAR) strategy, which is a simple, minimal effort and straightforward technique that appears in Fig. 1. (Pathan and Lokhande, 2004). The antecedent mixes utilized were ZnSO4.7H2O and FeSO4. 7H2O and NaOH are anything but difficult to deal with, economical and responsive compounds. The variables influencing the yield, morphology, molecule size and immaculateness of the nanocomposite have been assessed in this investigation. Basic refined water was utilized as a dissolvable for arrangement preparation, as a washing medium and as an anionic arrangement. Both the antecedent mixes utilized were white in shading (Chandramohan et al., 2013; Shampa, 2014).

Figure 7a & 7b

The Synthesized F doped CaZnO b) Growth of F doped CaZnO on a ceramic substrate

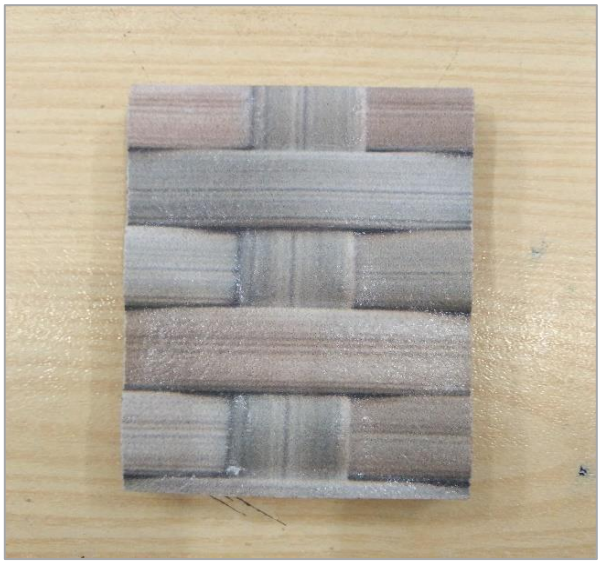

The Growth mechanism of F-doped CaZnO nanomaterial

Two vital advances are being made in the development component of Fe-doped ZnO nanomaterial on clay substrates. The initial step includes inundation of substrate (artistic) in the cationic antecedent; in this progression, the cations introduced in the arrangement were adsorbed on the surface of the substrate and, after that, unequivocally developed. The second substrate was plunged refined water that goes about as an anionic forerunner. In this stage, a concoction response happens, and the anions connect to the surface and shape the required compound on the

surface of the substrate. The refined water likewise expelled inadequately appended particles from the surface (Jose and Kumar, 2016)

Characterization of F-doped CaZnO nanomaterials

The following procedures were utilized to portray the orchestrated Fe-doped ZnO nanomaterial.

Characterization of Fe doped ZnO nanoparticle by X-beam Diffraction (XRD) procedure

An X-beam diffraction example of Fe-doped ZnO appears in Fig. 2. The number of pinnacles demonstrates that the Fe-doped ZnO test is exceptionally crystalline. The two theta esteems 35.6º,37.6º, 31.2º, 33.8º, 37.6º arrange the Miller records (100), (002), (101), (102), (110), (200), (112) and (201), individually that accommodated the readied item Fe doped ZnO (JCPDS no. 96-9004179). These qualities show that integrated Fe-doped ZnO tests have a hexagonal structure (Saba et al., 2017).

Figure 8

The XRD pattern of F-doped CaZnO nanoparticle

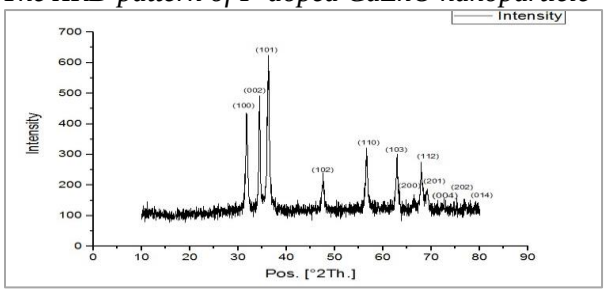

Figure 9A

The single unit cell

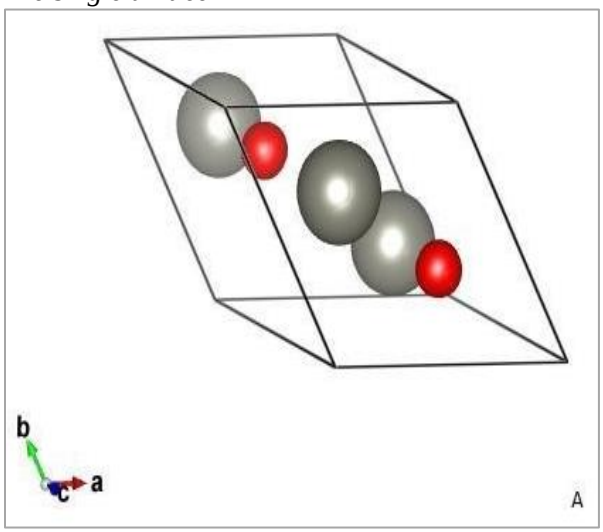

Figure 9b

The Multiple unit cell

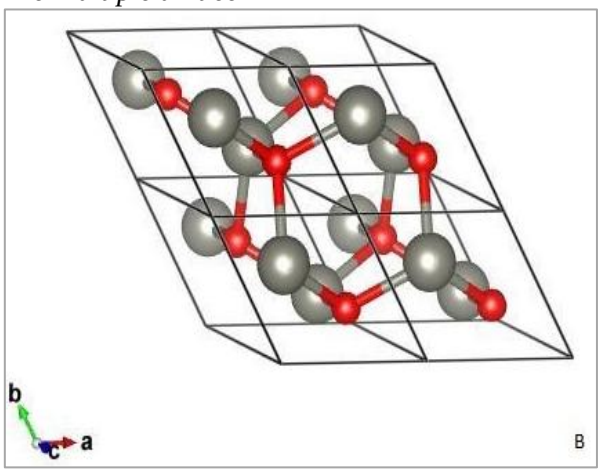

Figure 9C

The Three Specific Plans (100), (101) and (110)

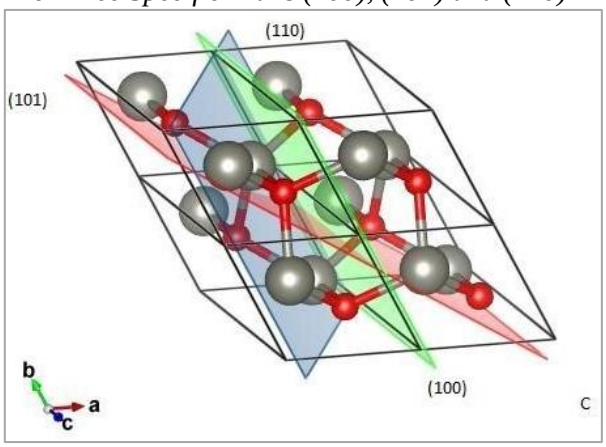

Table 2

Crystal information of XRD design figured from coordinate

Sr No	Parameters	Results
1	CRYSTAL SYSTEM	Hexagonal
2	SPACE GROUP	P 63 m c
3	DENSITY	5.68 g/cm3
4	CELL PARAMETER	
5	A, B and C (Aº)	3.25, 3.25 and 5.2
6	***α*, *β* and γ**	90, 90 and 120
7	X, Y, AND Z CO-ORDINATES OF O ATOM	0.333, 0.667 and 0.382
8	X, Y, AND Z COORDINATES OF Z ATOM	0.333, 0.667 and 0.00

Calculation of normal molecule measure

Gauge the normal molecule size of crystalline (L) of as-incorporated Fe doped ZnO can be computed with the assistance of Debye-Scherer′s Formula $L=k\lambda/\beta\cos\theta$ (Eq 4.1) Where, λ =1.54 Å k= 0.9 θ =

2θ/2 (from the chart) β= FWHM (from the chart), where β comparing to the full width at half most extreme pinnacle power (0.3022), L speaks to the normal precious stone size (in nm), and θ is a Braggs edge of diffraction. It has been uncovered that the normal precious stone size of combined material is 23.92 nm.

Energy Dispersive X-beam Analysis (EDX)

EDX affirmed the basic examination and virtue of the integrated example. The test has been accounted for to contain Zn, Fe, O and C in the EDX range, with three pinnacles of Zn having distinctive powers, three pinnacles of Fe, one pinnacle of oxygen and a little carbon. Zn was in higher focus contrasted with oxygen, suggesting the nearness of high substance of oxygen opportunities. Aside from unavoidable carbon, the non-appearance of some other components confirms the high virtue of the created nano-scaled Fe-doped ZnO (Nagarajan and Kuppusamy, 2013).

Figure 10

The Energy dispersive X-ray spectrum of synthesized F-doped CaZnO

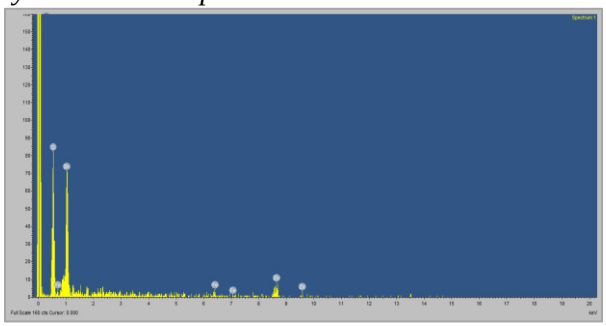

Table 3

Data of as-synthesized Fe doped ZnO by EDX

Sr. No	Element	Weight (%)	Atomic (%)
1	Oxygen (O)	0.68	44.47
2	Zinc (Zn)	0.97	49.64
3	Iron (Fe)	0.09	5.89
	Total	1.86	100

Scanning Electron Microscopy

The checking electron microscopy (SEM) estimation was completed with the goal of examining the structure and morphology of incorporated unadulterated examples. It has been observed that all the combined nanomaterials are permeable in nature and have a circular shape. The nearness of some greater particles may be ascribed to the collection or covering of smaller particles (Kaviyarasu and Devarajan, 2011).

Figure 11

The Scanning Electron Microscopics (SEM) Analysis of F-doped ZnO nanostructures

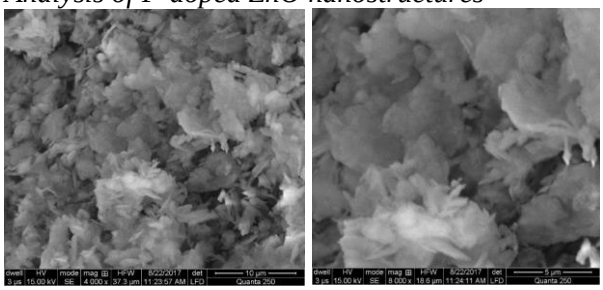

Evaluation of Humic substance (HS)/NOM from wastewater

The convergence of NOM in the example of wastewater was controlled by contrasting the standards of humic substances (HS). Standard arrangements of 20, 40, 60, 80 and 100 ppm were set up in 0.1 M KOH arrangement because humic corrosives are broken up in deionized water and looked at its assimilation at 254 nm (λmax). Draw a standard bend and look at the grouping of NOM in the example of wastewater. With the assistance of the standard, it was unmistakably demonstrated that the convergence of NOM in obscure wastewater test was 60 ppm, as appeared in Fig. no. 4.6. (Rodrigues et al., 2009)

Table 4

Absorbance of Standard Solution of HA

Concentration of HA	Absorbance at 254 nm
20	1.01
40	1.602
60	2.36
80	2.98
100	Non

Figure 12

The Quantification of NOMs with the help of standards

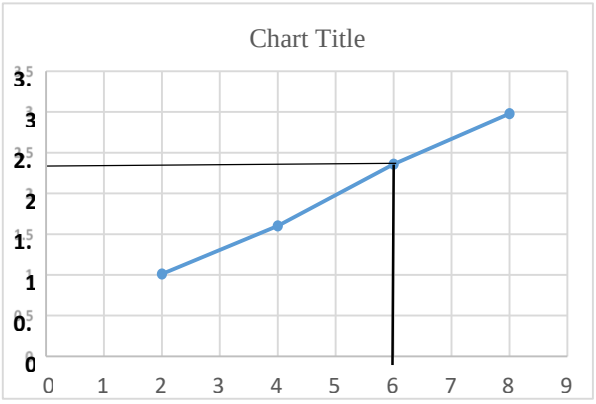

The Effect of Doping on Band Gap

Zinc oxide has interesting properties, such as photostability, photo activity, and syntheticity; however, it has an impediment in that it collects just in the UV locale. Doping is the marvels that conquer this impediment by expanding its capacity of ingestion into an unmistakable range, improving its photocatalytic proficiency, additionally creating section imperfection, for example, opportunities which assume a noteworthy part in the adjustment of physical and substance properties of oxide to a specific degree. In the work, ZnO doped Fe for the band hole's lessening; after that, the band hole was estimated by UV-vis spectrophotometry (Chandran et al., 2010).

Calculation of band hole vitality

Band hole vitality has been figured utilizing the accompanying condition Ebg(eV) = 1240/λ (nm) (Bhatkhande et al., 2002) Band Gap Energy (E) = hc/λ (Rajivgandhi et al., 2015)

Eg = (*hC*/λ) J = (*hC*/λe) eV

Where h =Plank's consistent (6.625x10-34J.sec) C =Velocity of light (3x108m/s) e =1.602x10-19J

1.602x10-19J = 1eVEg = (6.625x10^{-34}J.sec x 3x10^{8}m/s) ÷ (λ x 1.602x10^{-19})

Figure 13

Absorption spectrum of Fe doped ZnO nanostructure.

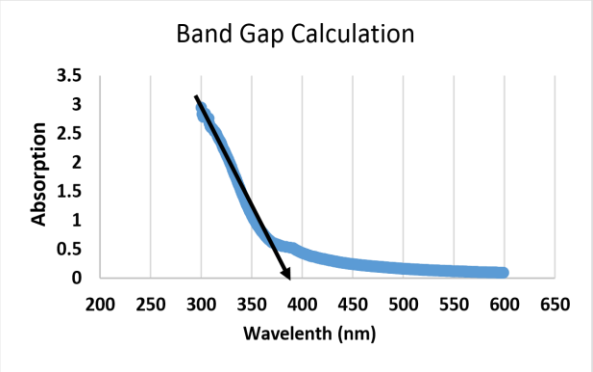

Eg = (6.625x10^{-34}J.sec x 3x10^{8}m/s) ÷ (393x10^{-9}m x 1.602x10^{-19})

Eg =3.15 eV

Degradation of Natural Organic Matter (NOM)

Wastewater contains many dangerous synthetic compounds, such as natural organic matter (NOMs), overwhelming metals, microorganisms, cleansers, and inorganic and natural synthetics. Common natural issue (NOM) is one of the major poisonous concoctions that cause the age of sterilization side-effects (DBPs), which are cancer-causing in nature. So, it is important to expel the NOM substance from water. Distinctive impacting parameters, for example, oxidant fixation, pH and time of illumination in regular daylight were improved before the corruption of NOM. (Chaudhary and Singh, 2014).

Statistical Design

The entire exploratory design for each keep-running examination is given below (Table). This demonstration empowers the analyst to perform experimentation under these chosen conditions, keeping in mind the end goal to expand astounding action in the notoriety of advanced conditions.

Table 5

Central composite design with predictive values and their experimental results.

Runs	pH	0xidant (H_2O_2) mM	Sunlight irradiation time Hour	Degradation Percentage
5	3.64	3.00	4.00	40
6	5.00	5.00	2.00	56
7	5.00	5.00	6.00	55
8	7.00	3.00	4.00	84
9	9.00	5.00	2.00	45
10	7.00	3.00	4.00	82
11	7.00	3.00	4.00	84
12	5.00	1.00	6.00	57
13	7.00	-0.36	4.00	46
14	7.00	3.00	0.64	35
15	9.00	1.00	2.00	52
16	7.00	3.00	7.36	84
17	7.00	6.36	4.00	70
18	10.36	3.00	4.00	43
19	9.00	1.00	6.00	48
20	7.00	3.00	4.00	85

Table 6

Sequential Model Sum of Squares

Source	Some of Squares	df	Mean Squares	F value	p-value prob > F	
Mean vs Total	76694.11	1	76694.11			suggested
Linear vs Mean	790.82	3	263.61	0.80	0.5103	
2FI vs. Linear	7.37	3	2.46	6.093E-003	0.9993	
Quadratic vs. 2FI	4416.22	3	1472.07	17.76	0.0002	suggested

Cubic vs Quadratic	818.68	4	204.67	122.29	< 0.0001	Aliased
Residual	10.04	6	1.67			
Total	82737.25	20	4136.86			

Table 7

Lack of Fit Tests

Source	Some of Squares	df	Mean Squares	F value	p-value prob > F	
Linear	5247.11	11	477.01	457.93	< 0.0001	
2FI	5239.73	8	654.97	628.77	< 0.0001	
Quadratic	823.51	5	164.70	158.11	< 0.0001	Suggested
Cubic4.83	1	4.83	4.64	0.0838	Aliased	
Pure Error	5.21	5	1.04			

Table 8

AN0VA table for Response Surface Quadratic Model Analysis of variance table [Partial sum of squares - Type III]

Sources	Some of Square	pdfs	Meen Square	F values	p-value probs > F	
Model	5214.42	9	579.38	6.99	0.0027	significant
A-pH	14.26	1	14.26	0.17	0.6870	
B-Time	638.88	1	638.88	7.71	0.0196	
C-h202	137.69	1	137.69	1.66	0.2264	
AB	0.12	1	0.12	1.508E-003	0.9698	
AC	1.13	1	1.13	0.014	0.9096	
BC	6.12	1	6.12	0.074	0.7913	
A2	3079.96	1	3079.96	37.17	0.0001	
B2	982.09	1	982.09	11.85	0.0063	
C2	1112.33	1	1112.33	13.42	0.0044	
Residual	828.72	10	82.87			
Lack of Fit	823.51	5	164.70	3.55	< 0.0001	Not significant
Pure Error	5.21	5	1.04			
Cor Total	6043.14	19				

Factors affecting photocatalytic degradation

Several factors govern dye photodegradation (Chong *et al*., 2010).

Interactive effect of Concentration of pH and Time

Figure 13 (a) Contour, (b)

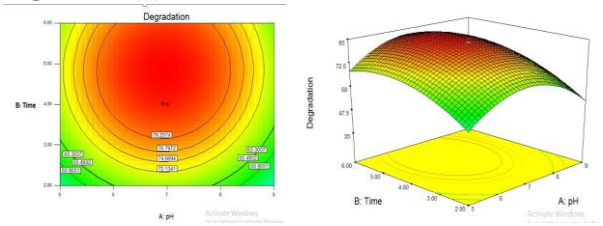

RSM of interactive the effect of pH and time on the degradation of NOM pH is a very sensitive factor that influences the degradation of natural organic matter (NOM). As the pH value increased from acidic to neutral, the degradation of NOM increased. If we increased the pH of the sample (wastewater), then degradation decreased. So, pH 7 is optimum for the degradation of NOM. Another factor is irradiation time, which reasonably affects NOM degradation. As the irradiation time increased from 2-4 hours, degradation also decreased, but after that, an irradiation time did not affect the degradation rate. So, pH seven and an irradiation time of 4 Hours are the optimum conditions for the degradation of NOM.

Interactive Effect of Concentration of H_2O_2 and Time

Figure 14 (a) Contour, (b)

RSM of the interactive effect of time and H_2O_2 on the degradation of NOM

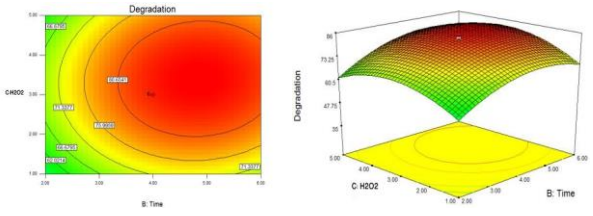

Irradiation time predominantly affects the rate of degradation. It has been shown that degradation increased as the irradiation time increased from 2

to 4 hours, after which removal efficiency became slow (Giahi et al., 2010). The degradation rate increased from 1 to 3 mM of H2O2 concentration, and further addition of H2O2 decreased the degradation to the extent that the irradiation time increased (Chong *et al*., 2010).

Interactive effect of Concentration of H_2O_2 and pH

Figure 15 (a) Contour, (b)

RSM of the interactive effect of pH and H_2O_2 on the degradation of NOM

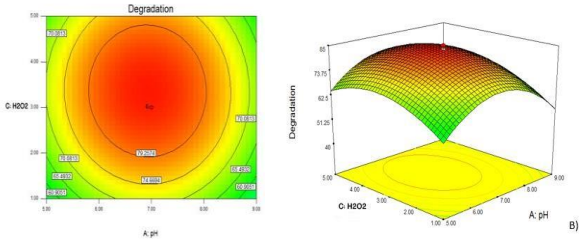

The effect of pH is also an important parameter in the degradation of NOM because it plays multiple roles. As pH relates to the surface of the catalyst by creating electron surface distribution on the surface of photocatalysts and organic compounds (NOM). From the literature, it is reported that catalytic activity in heterogeneous catalysis depends on the surface charge properties of the surface area. In lower pH, due to protonation, the catalyst's surface will be positively charged and act as Lewis acid, but on the other hand, due to anionic functional group on humic substance (HSs) and. In the case of alkaline conditions, this mechanism is not predominant due to a negative charge on the surface of the catalyst. Therefore, it causes the formation of the electrostatic force of repulsion between HSs/NOM and the catalyst's surface. The experimental results showed that the photocatalytic activity rises with increasing pH, ensuring the generation of more hydroxyl radicals toward high photocatalytic performance up to pH 7. Under neutral conditions, this compound provides the best degradation capability, as shown in 3D surfaces and contours (Rezaee *et al.*, 2014).

Degradation of Natural Organic Matter (NOM) in wastewater at lab scale

As shown in fig. no., NOM in the sewage sample was degraded in 4 hrs under the optimized condition, i.e., oxidant concentration (H2O2): 3 mM, pH of sample: 7 while catalyst loading, the concentration of NOM was kept constant.

Figure 16

Degradation of NOM at lab Scale

Degradation of Natural Organic Matter (NOM) in wastewater at lab scale

After degradation of NOM at lab scale, for the degradation of NOM at pilot scale, install a prototype inclined plan solar photocatalytic reactor having dimensions length: 6 feet, width: 4 feet and 20-degree angle that are shown in the fig. no. Run the experiment at the optimized condition as discussed above and determined the NOM at pilot scale. At the pilot scale, water was first collected in dram and stood overnight of the settle down of suspended/ undissolved materials. Then, transport water into another drain and recycle it with the help of a water pump, as shown in Fig. No.

Figure 17

Absorbance spectra of untreated municipal wastewater sample

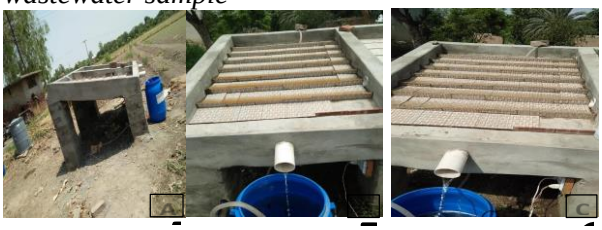

Figure 18

Pilot scale Degradation of Natural Organic Matter (NOM)

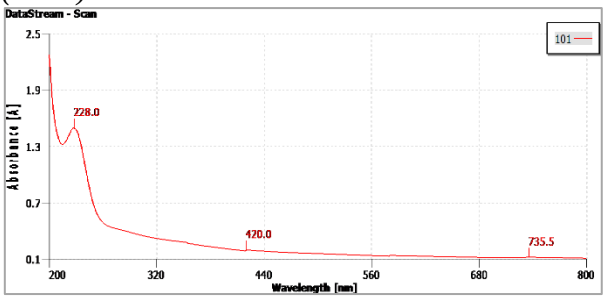

UV-Visible Spectrophotometry Analysis of Wastewater

UV-vis spectrophotometry confirmed natural organic matter (NOM) degradation in municipal wastewater. Characteristics of humic substances (HSs) can be explained with the help of UV-vis spectrophotometry. Absorbance at different wavelengths, such as absorbance at 254 nm, gives the idea of the total contents of humic substances (HSs); absorbance at 280 nm represents the total aromaticity of HSs. Absorbance at 400 and 436 nm represents the color removal for HSs. Differences in absorption also conformed to the degradation of NOM/HSs in wastewater samples. Absorbance spectra of untreated wastewater samples can be taken by scanning from 200 nm to 800 nm. This spectra peak near 254 nm confirmed the presence of NOM/HSs in the sample (Chamoli, 2013).

Figure 19

Absorbance spectra of treated sample

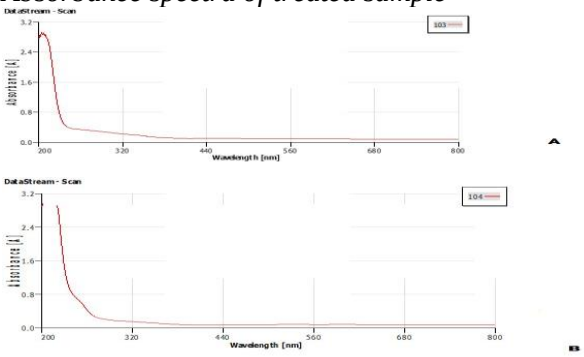

After photocatalytic treatment using Fe-doped ZnO, the contents of HSs/NOM were degraded, as shown in the spectrum of the treated sample. In the treated sample, near 254 nm, the peak of NOM/HSs contents disappeared, which conformed to the degradation of NOM/ HSs in the sample. **Fig: SUVA of Absorbance of NOM/HS at 254 nm**

Figure 20

Color Removal of NOM/HS

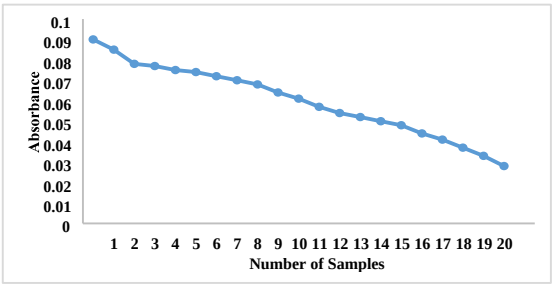

Fourier Transform Infrared Spectroscopy (FTIR) Analysis

The shape, position and intensity of an absorption band are helpful for the identification of functional groups in IR spectra. Position, intensity and shape of an absorption band are affected due to electron delocalization, electron-donating, withdrawing and hydrogen bonding. Natural Organic Matter (NOM) contains some major functional groups such as carboxylic-COOH, carbonyl-C=O, amine group, phenol-OH, C-H(sp3) and benzene ring that is shown in fig. 1, 2 and table 1. The peak appears between 3200-3700 cm^{-1} suggests the presence of NH group; the peak between 3200-3650 cm^{-1} indicates the presence of the OH group, the peak between 2850-3050 cm^{-1} suggests the presence of the C-H (sp3) group; peak between 1600-1800 cm^{-1} is indicated the presence of carbonyl-C=O group, and peak between 600-800 cm^{-1} is the peak of benzene ring but this peak shift below 600 cm^{-1} due different linkage with carboxyl-COOH, carbonyl-C=O etc that are shown in fig. no. 4.17 (Rodrigues *et al.*, 2009).

Figure 21

FTIR spectra of untreated wastewater sample

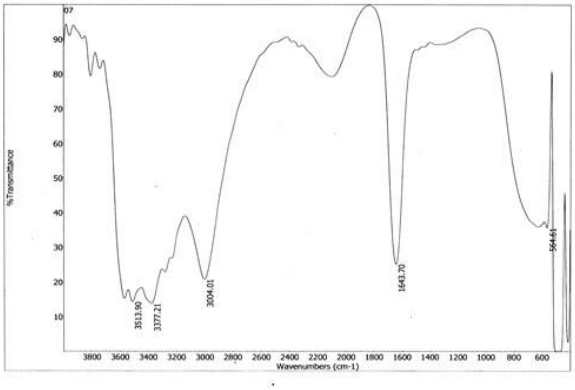

After treating wastewater with Fe/ZnO nanoparticles, it is indicated that a reasonable reduction in the intensity of all peaks conforms to the degradation of NOM from sewage. NH bond is less polar, so the absorption band for NH stretching is less intensive at 3463.3 cm^{-1}. The absorption peak appeared near 3800 cm^{-1}, the OH radical in water, so a new peak appeared at 3812.76, which is the peak of OH radical in water. Absorption at 2097.25 cm^{-1} suggested that a C-N functional group is present. Absorption at 689.92 cm^{-1} indicated the benzene ring was present (Chamoli, 2013).

Figure 22

FTIR spectra of treated wastewater sample

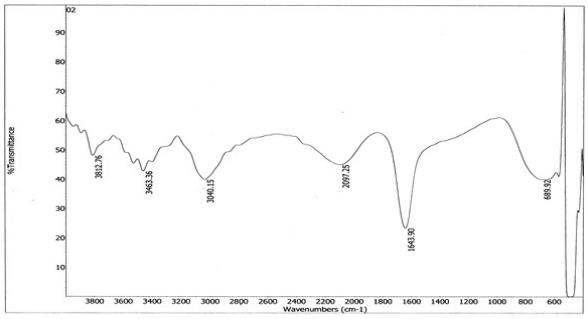

Table 9

COD of wastewater samples

Sr No.	Samples of WW	Degradation (%)
1	Residential WW	72
2	Municipal WW 1	76
3	Raja Wala Drain WW	68
4	Municipal WW 2	73

Figure 23

COD of untreated and treated wastewater samples

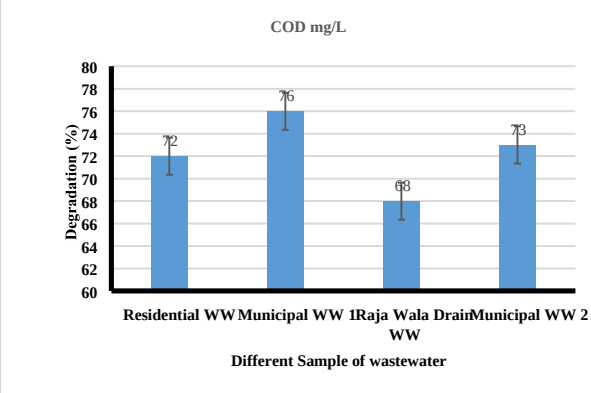

Reduction in BOD

The BOD values of wastewater standards were 433 mg/L before the treatment, which was reduced to 83 mg /L after photocatalytic treatment. The decrease in BOD values falls in the permissible range of water quality parameters

Table 10

BOD of wastewater samples

Sr No.	Samples of WW	Degradation (%)
1	Residential WW	72
2	Municipal WW 1	74
3	Raja Wala Drain WW	64
4	Municipal WW 2	71

After treatment, biochemical oxygen demand has been reduced to a great extent, as shown in the graph. (Fig. 4.23)

Figure 24

BOD values of wastewater before and after treatment using nano Fe doped ZnO

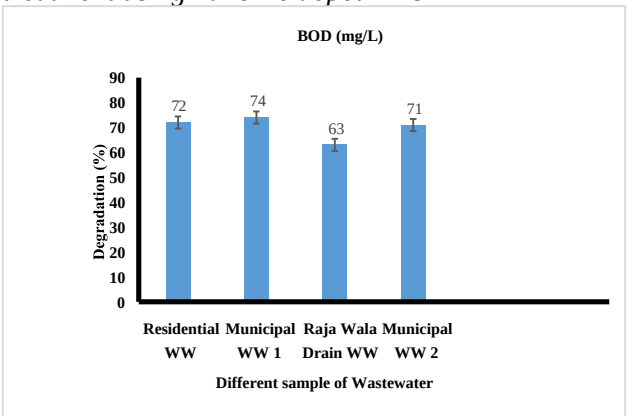

Reduction in TOC

Total organic carbon (TOC) present in different concentrations of wastewater samples has been measured before and after treatment. TOC is a key indicator of the organic pollution of water, as it measures the total amount of carbon in organic compounds. The reduction in TOC values after treatment indicates a decrease in the concentration of recalcitrant organic pollutants in the wastewater.

Table 11

TOD of wastewater samples

Sr No.	Samples of WW	Degradation (%)
1	Residential WW	35
2	Municipal WW 1	37
3	Raja Wala Drain WW	32
4	Municipal WW 2	39

Figure 25

TOD of untreated and treated wastewater samples

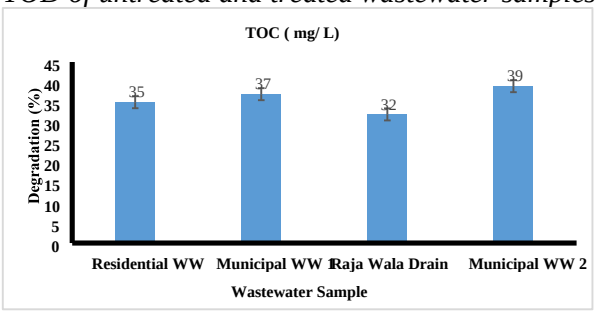

Reusability of Fe-doped ZnO nanoparticles

The material has been reused to check the photocatalyst's efficiency (Fe-doped ZnO nanoparticle). Results showed that Fe-doped ZnO nanoparticles could degrade the natural organic matter (NOM) in municipal wastewater samples. The functionalized substrate was reused twenty-two times in the present work to degrade the NOM

in municipal wastewater. Results showed that as the number of cycles increased, the efficiency of functionalized substrate retained continuously decreased. But even after use for twenty-two cycles, the functionalized substrate was able to degrade the pollutants up to more than 50%, as shown in the table as well as in the graph (Teixeira *et al*., 2016; Zhang *et al*., 2017)

Table 12

Reusability of Fe doped ZnO at lab Scale

Number of Cycles	Degradation (%)
1	81
2	85
3	84.5
4	85
5	85
6	85
7	84.5
8	84
9	85
10	83.5
11	81
12	79.5
13	74
14	72.5
15	70
16	67.5
17	62
18	60
19	56
20	54
21	52
22	51.5

Figure 26

Reusability of Fe doped ZnO at lab scale

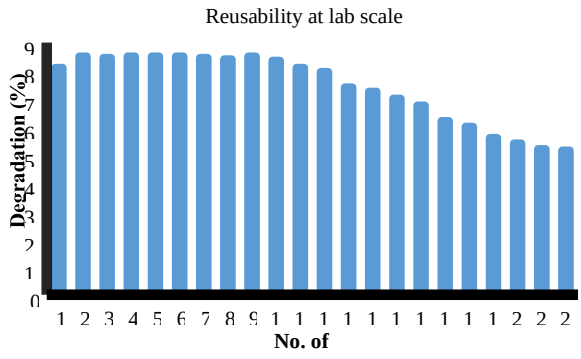

Table 13

Reusability of Fe doped ZnO at pilot Scale

No. of Cycle	Degradation (%)
1	63
2	69
3	68
4	63
5	59
6	57
7	54
8	51

Figure 27

Reusability of Fe doped ZnO at pilot scale Conclusion

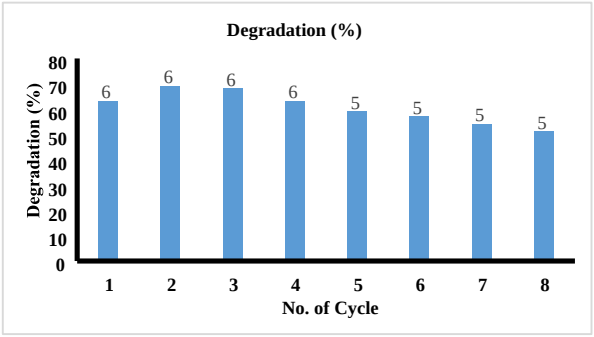

Water is one of the most important substances on the earth's crust; life does not exist without it. The shortage and proper supply of clean water sources have become a serious issue worldwide due to rapid population growth, industrialization and long-term droughts. Toxic chemicals such as Natural Organic Matter (NOMs), microorganisms, and inorganic and organic chemicals are present in high concentrations in wastewater. These contaminants change the chemical, biological and physical characteristics of water. In the present research, the fluorinated ZnO/CaO nanocomposite has been successfully grown on a gravel substrate using the spray pyrolysis method. Material characterization was accomplished by advanced analytical techniques such as X-ray diffraction (XRD), Scanning Electron Microscopy (SEM) and energy-dispersive X-ray (EDX). X-ray diffraction (XRD) pattern indicates the crystal size and structure of the different compounds; scanning Electron Microscopy (SEM) showed that rough and granular morphology and Energy Dispersive X-ray (EDX) exhibit the percentage purity and elemental analysis of the compound. Degradation was evaluated using UV-vis Spectrophotometry, Fourier Transform Infrared Spectroscopy (FTIR), and high-performance liquid chromatography (HPLC).

All our experiments were meticulously designed, incorporating the latest advancements in Response Surface Methodology (RSM) using central composite design (CCD). We used Design Expert 7 for this optimization method, conducting thirty experiments to fine-tune operational

parameters such as pH, irradiation time, oxidant concentration, and NOM concentration. Determining water quality parameters like BOD, COD, and TOC before and after treatment and the comprehensive assessment of material reusability using both lab and pilot scales underscore the thoroughness and reliability of our research methodology.

REFERENCES

Acero, J. L., Benitez, F. J., Real, F. J., & Teva, F. (2016). Micropollutants removal from retentates generated in ultrafiltration and nanofiltration treatments of municipal secondary effluents by means of coagulation, oxidation, and adsorption processes. *Chemical Engineering Journal*, *289*, 48–58. https://doi.org/10.1016/j.cej.2015.12.082

Ahmed, S. F., Mofijur, M., Nuzhat, S., Chowdhury, A. T., Rafa, N., Uddin, Md. A., Inayat, A., Mahlia, T. M. I., Ong, H. C., Chia, W. Y., & Show, P. L. (2021). Recent developments in physical, biological, chemical, and hybrid treatment techniques for removing emerging contaminants from wastewater. *Journal of Hazardous Materials*, *416*, 125912. https://doi.org/10.1016/j.jhazmat.2021.125912

Alatas, B., Akin, E., & Ozer, A. B. (2009). Chaos embedded particle swarm optimization algorithms. *Chaos, Solitons & Fractals*, *40*(4), 1715-1734. https://doi.org/10.1016/j.chaos.2007.09.063

Amini, M., & Ashrafi, M. (2016). Photocatalytic degradation of some organic dyes under solar light irradiation using TiO2 and ZnO nanoparticles. *Nanochemistry Research*, *1*(1), 79-86. https://doi.org/10.15242/ijacebs.u1016204

Andreozzi, R. (1999). Advanced oxidation processes (AOP) for water purification and recovery. *Catalysis Today*, *53*(1), 51-59. https://doi.org/10.1016/s0920-5861(99)00102-9

Anjum, M., Miandad, R., Waqas, M., Gehany, F., & Barakat, M. (2019). Remediation of wastewater using various nano-materials. *Arabian Journal of Chemistry*, *12*(8), 4897-4919. https://doi.org/10.1016/j.arabjc.2016.10.004

Anwar, Y., Khan, S., Hasan, S. W., Gamgali, A. R., Asif, M., Rahman, H. U., Ahmad, A., & Javed, M. S. (2024). Application of Nanostructured materials for the remediation of microbes contaminated water and sustainable water treatment. *Journal of Chemistry and Environment*, *3*(1). https://doi.org/10.56946/jce.v3i1.294

Ashar, A., Iqbal, M., Bhatti, I. A., Ahmad, M. Z., Qureshi, K., Nisar, J., & Bukhari, I. H. (2016). Synthesis, characterization and photocatalytic activity of ZnO flower and pseudo-sphere: Nonylphenol ethoxylate degradation under UV and solar irradiation. *Journal of Alloys and Compounds*, *678*, 126-136. https://doi.org/10.1016/j.jallcom.2016.03.251

Bethi, B., Sonawane, S. H., Bhanvase, B. A., & Gumfekar, S. P. (2016). Nanomaterials-based advanced oxidation processes for wastewater treatment: A review. *Chemical Engineering and Processing - Process Intensification*, *109*, 178-189. https://doi.org/10.1016/j.cep.2016.08.016

Borah, P., Kumar, M., & Devi, P. (2020). Types of inorganic pollutants: metals/metalloids, acids, and organic forms. In *Inorganic contaminants in water* (pp. 17-31). Elsevier.

Dad, A., Jeong, C. H., Wagner, E. D., & Plewa, M. J. (2018). Haloacetic acid water disinfection byproducts affect pyruvate Dehydrogenase activity and disrupt cellular metabolism. *Environmental Science & Technology*, *52*(3), 1525-1532. https://doi.org/10.1021/acs.est.7b04290

Hwang, T., Kotte, M. R., Han, J., Oh, Y., & Diallo, M. S. (2015). Microalgae recovery by ultrafiltration using novel fouling-resistant PVDF membranes with in situ PEGylated polyethyleneimine

particles. *Water Research*, *73*, 181-192. https://doi.org/10.1016/j.watres.2014.12.002

Imoberdorf, G., & Mohseni, M. (2011). Degradation of natural organic matter in surface water using vacuum-UV irradiation. *Journal of Hazardous Materials*, *186*(1), 240-246. https://doi.org/10.1016/j.jhazmat.2010.10.118

Kołodziejczak-Radzimska, A., & Jesionowski, T. (2014). Zinc oxide—From synthesis to application: A review. *Materials*, *7*(4), 2833-2881. https://doi.org/10.3390/ma7042833

Owodunni, A. A., & Ismail, S. (2021). Revolutionary technique for sustainable plant-based green coagulants in industrial wastewater treatment—A review. *Journal of Water Process Engineering*, *42*, 102096. https://doi.org/10.1016/j.jwpe.2021.102096

Podporska-Carroll, J., Myles, A., Quilty, B., McCormack, D. E., Fagan, R., Hinder, S. J., Dionysiou, D. D., & Pillai, S. C. (2017). Antibacterial properties of F-doped ZnO visible light photocatalyst. *Journal of Hazardous Materials*, *324*, 39-47. https://doi.org/10.1016/j.jhazmat.2015.12.038

Rajbongshi, B. M., & Samdarshi, S. (2014). Cobalt-doped zincblende–wurtzite mixed-phase ZnO photocatalyst nanoparticles with high activity in visible spectrum. *Applied Catalysis B: Environmental*, *144*, 435-441. https://doi.org/10.1016/j.apcatb.2013.07.048

RAJKUMAR, D., & KIM, J. (2006). Oxidation of various reactive dyes with in situ electro-generated active chlorine for textile dyeing industry wastewater treatment. *Journal of Hazardous Materials*, *136*(2), 203-212. https://doi.org/10.1016/j.jhazmat.2005.11.096

Rodriguez-Navarro, C., Burgos Cara, A., Elert, K., Putnis, C. V., & Ruiz-Agudo, E. (2016). Direct nanoscale imaging reveals the growth of calcite crystals via amorphous nanoparticles. *Crystal Growth & Design*, *16*(4), 1850-1860. https://doi.org/10.1021/acs.cgd.5b01180

Samanta, A., Chanda, D. K., Das, P. S., Ghosh, J., Mukhopadhyay, A. K., & Dey, A. (2015). Synthesis of Nano calcium hydroxide in aqueous medium. *Journal of the American Ceramic Society*, *99*(3), 787-795. https://doi.org/10.1111/jace.14023

Samudro, G., & Mangkoedihardjo, S. (2010). REVIEW ON BOD, COD AND BOD/COD RATIO: A TRIANGLE ZONE FOR TOXIC, BIODEGRADABLE AND STABLE LEVELS. *International Journal of Academic Research*, *2*(4).

Saravanan, A., Senthil Kumar, P., Jeevanantham, S., Karishma, S., Tajsabreen, B., Yaashikaa, P., & Reshma, B. (2021). Effective water/wastewater treatment methodologies for toxic pollutants removal: Processes and applications towards sustainable development. *Chemosphere*, *280*, 130595. https://doi.org/10.1016/j.chemosphere.2021.130595

Sharma, K., & Purohit, L. (2024). Solar light assisted enhanced photocatalytic activity of smart ternary ZnO:TiO2:SnO2 nanocomposites. *Materials Science in Semiconductor Processing*, *182*, 108671. https://doi.org/10.1016/j.mssp.2024.108671

Sievert, W., Altraif, I., Razavi, H. A., Abdo, A., Ahmed, E. A., AlOmair, A., Amarapurkar, D., Chen, C., Dou, X., El Khayat, H., ElShazly, M., Esmat, G., Guan, R., Han, K., Koike, K., Largen, A., McCaughan, G., Mogawer, S., Monis, A., … Negro, F. (2011). A systematic review of hepatitis C virus epidemiology in Asia, Australia and Egypt. *Liver International*, *31*(s2), 61-80. https://doi.org/10.1111/j.1478-3231.2011.02540.x

Singh, S., Barick, K. C., & Bahadur, D. (2013). Functional oxide nanomaterials and Nanocomposites for the removal of heavy metals and dyes. *Nanomaterials and Nanotechnology*, *3*, 20. https://doi.org/10.5772/57237

Tiwari, D. K., Behari, J., & Prasenjit Sen, P. S. (2008). Application of nanoparticles in waste water treatment. https://www.cabidigitallibrary.org/doi/full/10.5555/20083116147

Valencia, S. H., Marín, J. M., & Restrepo, G. M. (2012). Evolution of natural organic matter by size exclusion chromatography during photocatalytic degradation by solvothermal-synthesized titanium dioxide. *Journal of Hazardous Materials*, *213-214*, 318-324. https://doi.org/10.1016/j.jhazmat.2012.02.003

Westphall, C. B., Brunner, M., Nogueira, J. M., & Ulema, M. (2008). Pervasive management for ubiquitous networks and services—Report on NOMS 2008. *Journal of Network and Systems Management*, *16*(3), 317-321. https://doi.org/10.1007/s10922-008-9110-4